Subsurface and Atmospheric Influences on Solar Activity
ASP Conference Series, Vol. 383, ©2008
R. Howe, R. W. Komm, K. S. Balasubramaniam, and G. J. D. Petrie, eds.

On the Relationship Between CME-Associated Waves Observed on 5 March 2000

N.-E. Raouafi

National Solar Observatory, 950 N. Cherry Avenue, Tucson, AZ 85719, USA

D. Tripathi

Department of Applied Mathematics and Theoretical Physics, University of Cambridge, Wilberforce Road CB3 OWA, UK

Abstract. We study the relationship between different wave phenomena associated with a coronal mass ejection (CME) observed on 05 Mar. 2000. EIT waves were observed in the images recorded by EIT at 195 Å. The white-light LASCO/C2 images show clear deflection and propagation of a kink along with the CME. Spectroscopic observations recorded by the UVCS reveals excessive line broadening in the two O VI lines (1032 and 1037 Å). Moreover very hot lines such as Si XII and Mg X were observed. Interestingly, the EIT wave, the streamer deflection and the intensity modulation along the slit were all propagating northeast. Spatial and temporal correlations show that the streamer deflection and spectral line broadening are highly likely to be due to a CME-driven shock wave and that the EIT wave is the signature of a CME-driven shock wave in the lower corona.

1. Introduction

Coronal mass ejections (CMEs) are one of the most fascinating and intriguing forms of solar activity. They occur when solar plasma threaded with topologically complex magnetic fields are ejected out into the corona and interplanetary medium. Recent technological developments have yielded a steady increase in qualitative as well as quantitative studies of CMEs and related phenomena. However, numerous CME-associated phenomena such as the relationship between different wave features (EIT waves: Thompson et al. 1998; CME-driven shock waves: Hundhausen, Holzer, & Low 1987) are not understood unambiguously. CMEs with speed greater than the Alfvén speed of the local plasma produce shock waves whose effects can be traced through radio type II bursts (Klassen et al. 2000) and/or emission of very hot lines (compared to the ambient coronal temperatures; Raouafi et al. 2004). These waves could also be detected through deflections in remote streamer belts with respect to the ejected CME material (see Hundhausen et al. 1987 and Sime & Hundhausen 1987). The high quality data of SOHO/LASCO (Brueckner et al. 1995) yielded numerous cases for streamer deflections associated with super-Alfvénic CME eruptions (Sheeley, Hakala, & Wang 2000). These observations led to the conclusion deduced by the previous authors that these deflections were indeed a consequence of CME-driven shock waves.

Spectroscopic signatures of coronal shock waves due to high speed CMEs (> 600 km s^{-1}; see Raymond et al. 2000) are line broadening (e.g., O VI 1032 Å and 1037 Å lines) and enhanced emissions in spectral lines that are rarely observed in the corona such as Si XII 520 Å and Mg X 625 Å (e.g., Raouafi et al. 2004) due to their relatively high formation temperatures (> 2 MK). Up to now only a few CME-driven shock wave events have been reported through SOHO/UVCS (Kohl et al. 1995) observations: Raymond et al. (2000); Mancuso et al. (2002); Raouafi et al. (2004); and Ciaravella et al. (2005) (hereafter RMRC00-05).

Since the discovery of the Hα Moreton waves (Moreton 1964), it was thought that these waves were due to the intersection of coronal shock waves (due to flares) with the chromosphere (e.g., Uchida 1968) when EIT waves (Thompson et al. 1998) were discovered based on the observations recorded by EIT (Delaboudinière et al. 1995), they were interpreted as the coronal manifestation of the chromospheric Moreton wave (Thompson et al. 1999). However, the difference in propagation patterns and speeds of Moreton and EIT waves questions the similarity between these two phenomena.

Although these waves are being observed more frequently the question remains open as to how these different wave phenomena are related to each other. Based on MHD simulations, (Chen, Fang, & Sabata 2005a; Chen, Ding, & Fang 2005b) showed that Moreton waves are the surface counter part of the CME driven shock wave. However, the EIT waves are the slow moving wave fronts traveling behind the Moreton wave due to the opening of the magnetic flux system. This was also suggested by Zhukov & Auchère (2004) and by Delannée (2000). However, this relationship and the nature of EIT waves remains elusive.

A CME event on 5 March 2000 has been observed simultaneously by different instruments on board SOHO (EIT, LASCO and UVCS) with different signatures of wave features. This event provides a unique opportunity to establish a relationship between different phenomena such as the CME driven shock wave, streamer deflection and the EIT waves. Observations and data analysis are described in §2 and results and conclusions are presented in §3.

2. Observations, Data Analysis and Results

2.1. LASCO Observation of the CME and streamer deflection

The CME event of 5 March 2000 appeared as a three-part structure (bright front followed by a dark cavity and a bright core) in the LASCO/C2 field of view (FOV) at 16:54 UT. Images with FOV extending from 2.5–6.0 $R_\odot$ were recorded every 20 minutes. Figure 1 displays the running difference of LASCO/C2 images of the white-light CME showing the proper motion of features (Sheeley et al. 2000). The bright material seen as a core of the CME is the erupting prominence which had expanded. The leading edge of the CME propagated with a super Alfvénic speed of 860 km/s (Tripathi et al. 2006).

The arrows mark the location of the streamer deflection propagating northeast. As depicted in Figure 1, there is no evidence of plasma material which could have caused such a kink in the streamer. The simultaneous propagation of the kink in the streamer outward in the corona along with the CME provides strong evidence for the existence of a wave phenomenon traveling in the flank of the CME. The speed of the propagating kink (projected on the plane of the

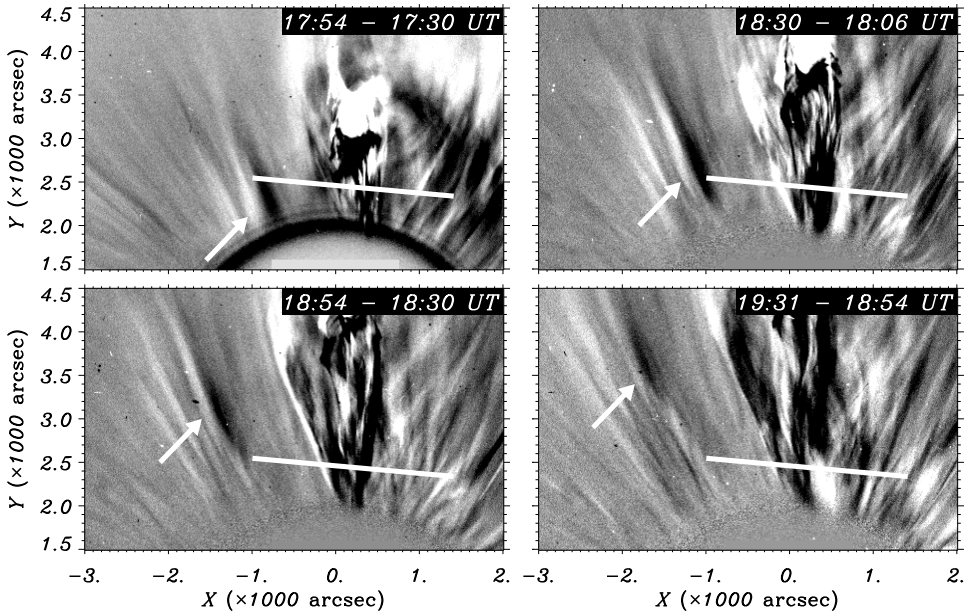

Figure 1. Running difference of LASCO-C2 white-light images. The arrows locate the propagating kink in the streamer. The location of the UVCS slit is shown by the white straight line.

sky), measured by tracking the boundary between the bright and dark features from the running difference images, was about 260 km s^{-1}. Sheeley et al. (2000) found that speed of the CME-flank material is likely to be smaller than that of the bright leading edge (860 km s^{-1} in the present case). Since the CME propagates with super-Alfvénic speed, it can drive a shock. Therefore it is plausible to conclude that the propagating kink was likely to be the consequence of shock wave driven by the associated CME.

2.2. UVCS Observations

The UVCS observational sequence started at 15:58 UT and ended at 20:12 UT. This time interval covers adequately the time evolution of the CME event that first appeared in the LASCO at around 16:54 UT. The 40 arcmin long UVCS slit was centered at 2.55 $R_\odot$ from Sun center at 355° counterclockwise (CCW) from the North pole. 80 exposures of 180 seconds each have been recorded in the wavelength ranges of 1027–1042 Å and 1241–1253 Å for the main and redundant channels, respectively. The latter includes the Mg X 625 Å line (observed in second order), where the former contains the strong O VI doublet 1032 Å & 1037 Å together with other weaker lines such as Si XII 520 Å which is observed in second order. However, we concentrate on the first 21 exposures where hot plasma emission is observed before the CME material has reached the slit.

Figure 2 displays two sets of averaged UVCS exposures (top panel: average of exposures from 1 to 15; bottom panel: average of exposures from 16 to 21) showing the O VI doublet together with the Si XII 520 Å line. The overplotted spectra are spatially binned between the two horizontal lines plotted on the

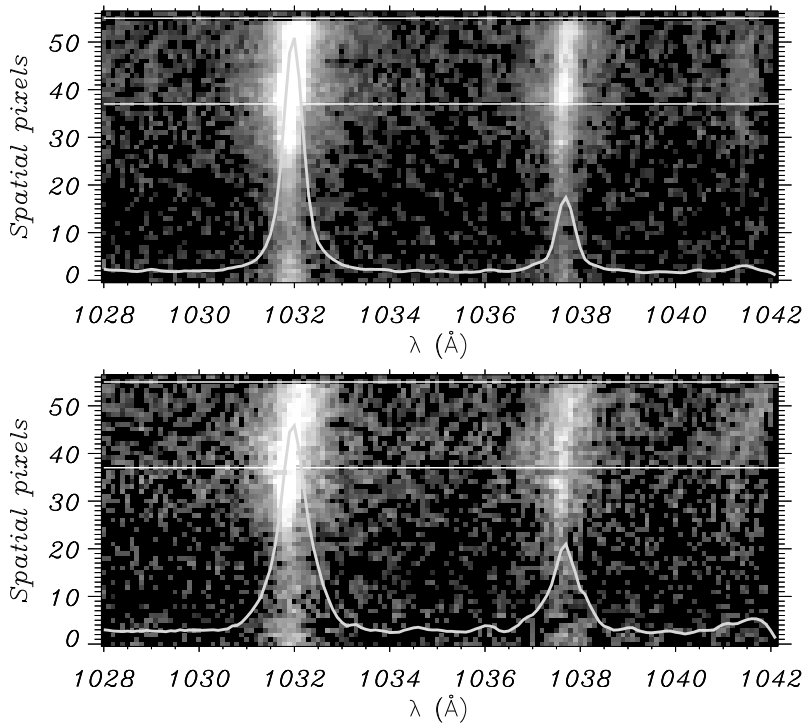

Figure 2. Averages of exposures 1–15 (top) and 16–21 (bottom) of the UVCS observation sequence of 5 March 2000 at 15:58 UT. The spectral lines shown are the O VI doublet at 1032 Å and 1037 Å and the weak line of Si XII at 520 Å observed in second order. The spectra overplotted on each panel are the corresponding spatially-binned ones between the two horizontal lines. The focus is on the shape of the profiles and then the amplitudes of the profiles are indirectly proportional to the real ones.

figure. Note that the amplitude of the spectral lines are not to scale and only the change in the profile shapes are emphasized. The O VI line profiles in the top panel are composed mainly of a central narrow component and emission in the Si XII line is weak but remarkable. In the bottom panel, the O VI lines are dimmed compared to the previous one and are significantly wider as shown by the overplotted spectra. The emission profiles in the Si XII line are enhanced and are also wider.

Figure 3 shows the average of the first 21 exposures in the redundant channel covering the Mg X 625 Å (second order). The spatially binned spectra between the horizontal lines are overplotted. The solid curve is the spatially binned spectra of all the 21 exposures. The significance of the other curves is explained in the caption of the same figure. The dot-dashed spectrum (average of exposures 16–21) shows an intensity enhancement and profile broadening of the Mg X line simultaneously with the broadening of the O VI and Si XII lines.

The increase in the line widths together with enhanced emissions in hot lines are very likely due to plasma heating which is very likely due to a shock wave propagating in front of the CME (e.g., Raouafi et al. 2004 and RMRC00-05). A simple time computation suggested that the shock wave has reached the

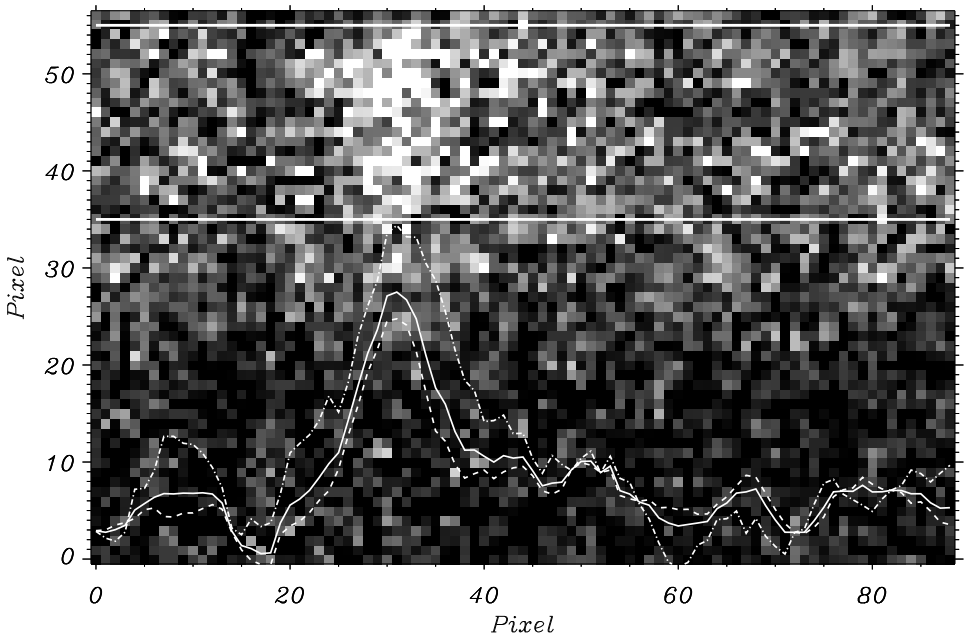

Figure 3. Average of the first 21 exposures recorded in the redundant channel of the UVCS telescope showing an intensity enhancement of the Mg X 625 Å line. The normalized spectra averaged over spatial bins between the two horizontal lines are overplotted (solid: exposures 1–21; dashes: 1–15; dot-dashes: 16–21). Note the intensity enhancement and the excessive broadening of the Mg X line in the exposures 16–21, which occurs simultaneously with the broadening and intensity enhancement of the O VI and Si XII lines (see Fig. 2).

UVCS slit after 16:45 and the heated gas emission lasted till about 17:20 UT, where emission in colder lines is observed. Extra broadening in the O VI lines is noticeable even after the CME cold material has reached UVCS FOV. The intensity modulation along the slit, in particular the upper section of the slit, shows structures drifting towards the upper end of the slit, which corresponds to the northeast direction (see Tripathi & Raouafi 2007). In addition, intensity dimming in the upper section of the slit of the O VI 1032 Å line from one exposure to the next, where that of the 1037 Å line changes quite differently. It gets enhanced in particular in exposure number 20. This is evidence for the acceleration of the O VI ions that leads the 1032 Å line to run out of resonance and the 1037 Å line to get optically pumped by the chromospheric lines of C II. We believe that is evidence that the physical process causing the intensity variation and lines' broadening (as shown previously) is moving along the slit to the northeast quadrant of the solar corona.

2.3. EIT Observations: EIT Wave

SOHO/EIT images at 195 Å are recorded regularly with a cadence of 12 mins and were used for the present study. Figure 4 displays the running difference images taken by EIT at 195 Å. The filament slowly rose and erupted at 15:46 UT.

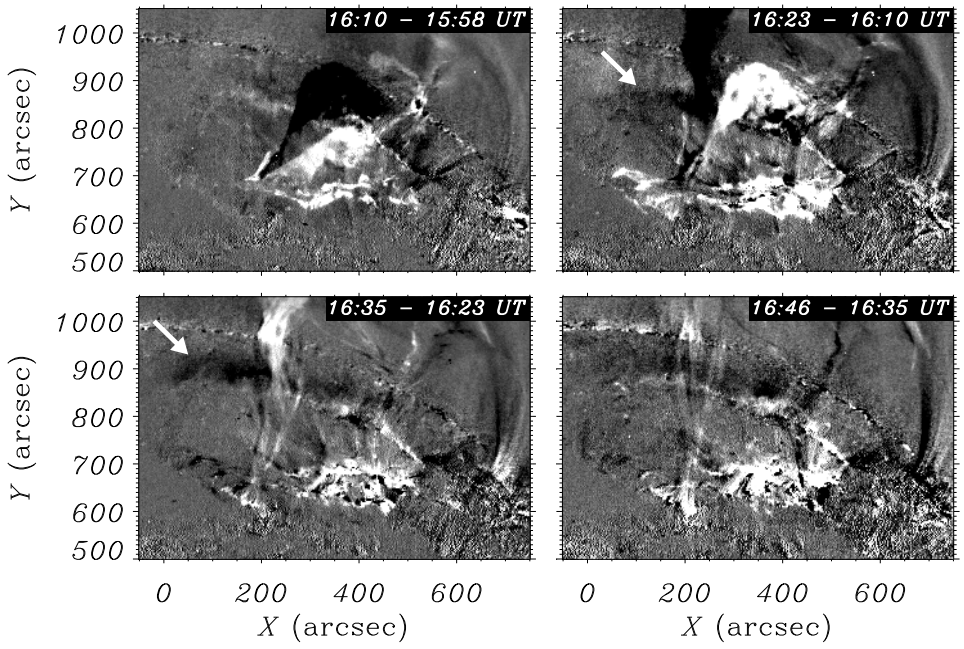

Figure 4. EIT running difference images showing the EIT waves. Arrows locate the EIT wave front.

The EIT wave associated with this eruption first appeared at 16:10 UT and disappeared at 16:58 UT.

The EIT wave is seen propagating only towards the northeast. No counterpart moving to the southwest was detected probably because of the presence of an active region. The propagating wave-front also did not traverse through the coronal hole which was located northeast of the source region, similar to the observations presented by Thompson et al. (1999). The estimated average speed of the propagation was about $55\,\mathrm{kms}^{-1}$. Note that no correction for the projection effect was performed while measuring the speed. Except for the speed being much lower, other characteristics are similar to those of the EIT waves.

3. Summary of Results and Discussion

We studied the relationship between different coronal waves (EIT wave, streamer deflection and a CME-driven shock wave) generated by the CME event on 5 March 2000 as observed by different instruments on board SOHO (EIT, LASCO and UVCS).

LASCO-C2 images show a deflection propagating outward at ~ 260 km s^{-1} (projected on the plane of the sky) in a remote streamer located approximately at $10^\circ - 15^\circ$ CCW from the North pole. The streamer kink was first seen in LASCO-C2 FOV (~ 2.5 R$_\odot$) at about 17:30 UT. No evidence for any CME material which could be the origin of such a deflection. The speed of the leading edge of the CME was ~ 860 km s^{-1}, which is sufficient to generate a shock wave.

Therefore, this propagating kink in the streamer provides strong evidence for a CME-driven shock wave in the corona as suggested by Sheeley et al. (2000).

UVCS spectra show excessive broadening in O VI lines and intensity enhancement in the hot lines of Si XII 520 Å and Mg X 625 Å. These are clear evidence for a CME-driven shock wave (see RMRC00-05). The analysis of the intensity modulation along the slit also reveals the propagation direction of the wave, northeast, that is the same as the kinking streamer. UVCS observations show that the shock wave would have reached the UVCS slit around 16:45 UT.

EIT difference images show evidence for an EIT wave front propagating northeast with a speed of $\sim 55\,\mathrm{kms}^{-1}$ (the solar disk shape not taken into account) up to the North polar hole where the propagation has stopped, satisfying the properties of EIT waves. The propagation of the wave in the southeast direction seems to be disabled by the presence of the complex active region. The EIT wave first appeared at 16:10 UT and disappeared gradually after 16:58 UT.

On one hand, temporal and spatial correlations between the events observed by UVCS and LASCO suggest that they are basically different manifestations of the same phenomenon. Measurements of the speed in different part of CME envelopes reveal that noses of CMEs travel faster than their flanks (Sheeley et al. 2000). Therefore we anticipate that the propagating shock would have a similar property and would have speed higher in front of the CMEs and lower in the flanks. Different speed in the different parts would provide evidence for the anisotropic propagation of associated shock waves. On the other hand, the EIT wave observed in the low corona was significantly slower than the UVCS and LASCO events. A possible explanation for this is the opening of the magnetic flux system due to the expulsion of the CME rather than the manifestations of the CME driven shock wave as suggested by Chen et al. (2005a,b) based on MHD modeling and by Delanee (2000) and by Zhukov & Auchère (2004). Moreton waves, which are observed in the chromosphere, are interpreted as the counterpart of CME driven shock waves (e.g., Chen et al. 2005a). Unfortunately, we did not have Hα high cadence observations for this event, which prevented a comparison with a chromospheric Moreton wave. However, the semi-circular wavefront was moving in the same direction as the coronal shock wave. This supports the hypothesis that all three features are linked to each other. They are generated by the same source, propagate in the same direction and have good time and spatial correlations. The only apparent problem resides in the propagation speed. However, note that the three wave-like structures do not share similar physical conditions. One of these is the space and its characteristics. The speed of Alfvén waves is given by $V_A = B/\sqrt{4\pi\rho}$, where B is the magnetic field strength and ρ is the density. Depending on models, the density drops by 3 to 4 orders of magnitude or more between the very sparse corona and 2.0–3.0 $\mathrm{R}_\odot$, where the magnetic field drops by an order of magnitude or more (assuming that the coronal field is nearly potential and thus drops as r^{-2}; see Altschuler & Newkirk 1969). While the high corona is increasingly less dense with increasing altitude the corresponding Alfvén speed tends to increase. This is not the case in the lower corona where the plasma density is higher and thus is characterized by a smaller Alfvén speed. This may explain at least partially the difference in speed. Another parameter is the propagation direction of the waves. The CME-driven shock wave is mainly propagating parallel to the mag-

netic field lines. However, the wave propagating on the solar disk does not share this property and propagates across. It encounters different magnetic structures that may allow for energy leakage which might consequently damp and slow down the wave (see for instance De Pontieu et al. 2004 on energy leakage of the acoustic oscillation p modes through flux tubes with high inclinations to the chromosphere, which contributes to the heating of this layer). A good illustration for that is given by active regions through which EIT waves could not propagate and also across polar holes. We think that energy carried by the wave is progressively leaked to different magnetic structures which may heat and accelerate the plasma in these structures. This interpretation needs to be carried further and deeper through additional analysis of other observational examples and also by numerical simulations.

Acknowledgments. The National Solar Observatory is operated by the Association of Universities for Research in Astronomy, Inc., under cooperative agreement with the National Science Foundation. NER's work is supported by NSO and NASA grant NNH05AA12I. DT acknowledges the support from STFC. SOHO is a project of international collaboration between ESA and NASA.

References

Altschuler, M. D., & Newkirk, G., Jr. 1969, Solar Phys., 9, 131
Brueckner, G. E., Howard, R. A., Koomen, M. J., et al. 1995, Solar Phys., 162, 357
Ciaravella, A., Raymond, J. C., Kahler, S. W., et al. 2005, ApJ, 621, 1121
Chen, P. F., Fang, C., & Shibata, K. 2005a, ApJ, 622, 1202
Chen, P. F., Ding, M. D., & Fang, C. 2005b, Space Sci.Rev., 121, 201
Delannée, C. 2000, ApJ, 545, 512
Delaboudinière, J.-P., Artzner, G. E., Brunaud, J., et al. 1995, Solar Phys., 162, 291
De Pontieu, B., Erdélyi, R., & James, S. P. 2004, Nat, 430 536
Hundhausen, A. J., Holzer, T. E., & Low, B. C. 1987, J. Geophys. Res., 92, 11173
Klassen, A., Aurass, H., Mann, G., & Thompson, B. J. 2000, A&AS, 141, 357
Kohl, J. L., Esser, R., Gardner, L. D., et al. 1995, Solar Phys., 162, 313
Mancuso, S., Raymond, J. C., Kohl, J., et al. 2002, A&A, 383, 267
Moreton, G. F. 1964, AJ, 69, 145
Raouafi, N.-E., Mancuso, S., Solanki, S. K., et al. 2004, A&A, 424, 1039
Raymond, J. C., Thompson, B. J., St. Cyr, O. C., et al. 2000, Geophys. Res. Lett., 27, 1439
Sime, D. G., & Hundhausen, A. J. 1987, J. Geophys. Res., 92, 1049
Sheeley, N. R., Hakala, W. N., & Wang, Y.-M. 2000, J. Geophys. Res., 105, 5081
Thompson, B. J., Plunkett, S. P., Gurman, J. B., et al. 1998, Geophys. Res. Lett., 25, 2465
Thompson, B. J., Gurman, J. B., Neupert, W. M., et al. 1999, ApJ, 517, L151
Tripathi, D., Solanki, S. K., Schwenn, R., et al. 2006, A&A, 449, 369
Tripathi, D., & Raouafi, N.-E. 2007, A&A, 473, 951
Uchida, Y. 1968, Solar Phys., 4, 30
Zhukov, A. N., & Auchère, F. 2004, A&A, 427, 705